The effective shielding of $NaYF_4:Yb^{3+},Er^{3+}$ upconverting nanoparticles in aqueous environments using layer-by-layer assembly.

Emilia Palo[*⊥,†,‡], *Satu Lahtinen*[*⊥‖], *Henna Päkkilä*[‖], *Mikko Salomäki*[†,§], *Tero Soukka*[‖], *and Mika Lastusaari*[†,§]

[†] University of Turku, Department of Chemistry, FI-20014 Turku, Finland

[‡] University of Turku Graduate School (UTUGS), Doctoral Programme in Physical and Chemical Sciences, Turku, Finland

[§] Turku University Centre for Materials and Surfaces (MatSurf), Turku, Finland

[‖] University of Turku, Department of Biochemistry, FI-20014 Turku Finland

Corresponding author

* emilia.palo@utu.fi, satu.elina.lahtinen@utu.fi

[⊥] Authors had equal contribution

KEYWORDS: layer-by-layer; polyelectrolytes; lanthanides; nanoparticles; upconversion luminescence

ABSTRACT

Aqueous solutions are the basis for most biomedical assays but they quench the upconversion luminescence significantly. Surface modifications of upconverting nanoparticles are vital for shielding the obtained luminescence. Modifications also provide new possibilities for further use by introducing attaching sites for biomolecule conjugation. We demonstrate the use of layer-by-layer surface modification method combining varying lengths of negatively charged polyelectrolytes with positive neodymium ions in coating the upconverting $NaYF_4:Yb^{3+},Er^{3+}$ nanoparticles. We confirmed the formation of the bilayers and investigated the surface properties with FT-IR and reflectance spectroscopy, thermal analysis and zeta potential measurements. The effect of the coating on the upconversion luminescence properties was characterized and the bilayers with the highest improvement in emission intensity were identified. In addition, studies for the nanoparticle and surface stability were carried out in aqueous environments. It was observed that the bilayers were able to shield the materials luminescence from quenching also in the presence of phosphate buffer which is currently considered the most disruptive environment for the nanoparticles.

INTRODUCTION

Materials exhibiting upconversion luminescence[1] have been studied intensively for the last decade because of their potential use in photovoltaics,[2,3] biomedical imaging and theranostics,[4–6] and in biomedical assays.[7–9] Especially the research in the biomedical field has benefitted from the extensive development of upconversion material syntheses resulting in nanoscale materials down to 5 nm.[10–13] Currently, hexagonal β-$NaYF_4:Yb^{3+},Er^{3+}$ is considered to be the most efficient material in upconversion.[14,15] Its superiority is thought to arise from the low phonon energy in

fluoride lattice[16] as well as shorter R-R distance compared to the cubic structure of $NaYF_4:Yb^{3+},Er^{3+}$. [17] While the unique properties of upconversion nanoparticles have advantage in the biomedical applications such as less scattering of light, photodamage of tissue and minimal autofluorescence they still have drawbacks that need to be solved.[18]

One of the most critical problems of upconverting nanoparticle use in biomedical applications is the significant quenching of the upconversion luminescence in aqueous environment due to OH^- vibrations in water.[19] Additional processing steps are commonly required to obtain water dispersible materials, as most of the syntheses result in hydrophobic particles.[11,18] Furthermore, undesired disintegration of the used nanoparticles has been observed in water and in various aqueous buffers being the most prominent in phosphate buffer.[20,21] So far it is unclear which contributes most into emission intensity decrease in aqueous environment, the quenching of upconversion luminescence through ytterbium on the surface or the disintegration of the whole nanoparticle. One method of improving the emission intensity in aqueous environments is to produce more efficient materials. This has been made possible for example with core-shell structures[22,23] or using plasmonic enhancement.[24,25] However, especially in the cases where the shell is composed from similar fluoride structure as the core it could be debated that it is also vulnerable to the disintegration mentioned previously. Recently, an amphiphilic coating was demonstrated to be successful in hindering the disintegration and thus shield the particles' luminescence from quenching.[26] Preventing the disintegration of the materials is vital, not only because of the optical changes harming the reproducibility of the measurements[20,21] but also because preventing the leaking of lanthanide and fluoride ions into the tissue or living cells in biomedical imaging.[27,28] This means that development of new surface modifications and methods

to effectively stop the disintegration are increasingly important topic for the research of upconverting nanoparticles.

Our aim was to study the shielding of the upconverting nanoparticles with layer-by-layer (LbL) method[29–32] and how varying the length of the polyelectrolyte (PE) chain affects the surface coating and luminescence properties. The layer-by-layer method has not been fully researched previously with upconverting nanoparticles and can provide multiple new insights into their surface modifications. Commonly, oppositely charged polyelectrolytes are used in forming the bilayers but it is also possible to use inorganic components such as positive metal ions.[33,34] The studied $NaYF_4:Yb^{3+},Er^{3+}$ nanoparticles were coated with negatively charged polyelectrolyte and positively charged neodymium ions to produce bilayers. The negatively charged polyelectrolyte is expected to attach on the nanoparticle surface similarly via carboxyl or phosphate group as when coated with oleic acid. After the first negative polyelectrolyte layer the buildup of bilayer coating is reached by varying the charge of the deposited layer.[35] Both poly(acrylic acid) (PAA) and polyphosphate (PP) were used as polyelectrolytes and neodymium was chosen as positive ion because of its easy optical detection from bilayers and from the lanthanide ions at the core. Neodymium could also be used as a possible sensitizer for 808 nm excitation.[36,37] The coating with varying polyelectrolyte molecular weight (and thus length) and its coverage was studied with small number of bilayers (1-3) due to previous observation that the advantage of shielding the core material and improving the luminescence seems to weaken after three bilayers.[35] The formation of the bilayers was studied with appropriate methods such as FT-IR and reflectance spectroscopy to observe deposited polyelectrolytes and neodymium ions, respectively. Thermal analysis was used to give further insight on to the bilayer formation and zeta potential to observe changes on the surface. Upconversion luminescence measurements were made to powder materials using 973 nm

excitation at power range of 3.2–11.1 Wcm^{-2} to observe the changes in obtained emission due to the coating of the materials. In addition, upconversion luminescence decay and the stability of the nanoparticles with bilayers was investigated in aqueous suspensions observing the emission intensity at selected time intervals using 980 nm excitation.

MATERIALS AND METHODS

Reagents.

Poly(acrylic acid) (PAA; $M_w \approx$ 2,000; 15,000 or 100,000), $(C_3H_4O_2)_n$, Aldrich), potassium polyphosphate (PP; long chain, potassium metaphosphate $(KO_3P)_n$, ABCR; short chain, sodium polyphosphate $(NaPO_3)_n$), sodium chloride (NaCl 99.5 %, J.T. Baker), neodymium(III) chloride hexahydrate (99.9 % purity with respect to other rare earths, Sigma-Aldrich). Absolute ethanol was used as received. 5 mM phosphate buffer pH 7.75 and potassium fluoride (KF 99 %, Merck) were used for the decay measurements along with Greiner polypropylene microtiter plate (Sigma-Aldrich).

Materials preparation.

The β-$NaYF_4$:Yb^{3+},Er^{3+} (x_{Yb}: 0.17, x_{Er}: 0.03) nanoparticles (size *ca*. 22*26 nm) used as a core material were prepared with the synthesis procedure reported previously[13] and the oleic acid present at the nanoparticle surface was removed with previously described acidic treatment before coating.[35,38] The coating solutions contained 10 mM PAA/PP (referring to monomer concentration of the polyelectrolyte) solubilized in 0.1 M NaCl(aq) and 10 mM $NdCl_3 \cdot 6H_2O$ in quartz distilled H_2O. The pH of the solutions was unadjusted *ca.* 5.

The coating cycle of the nanoparticles was the same as reported previously.[35] The core particles (*ca.* 50 mg) were dispersed into coating solution and ultrasonicated for two minutes and washed with quartz distilled water twice to remove any excess unattached material to prepare half a bilayer. For the aqueous measurements an additional layer of PAA (the length of polyelectrolyte being equal to those that used in the bilayers in PAA and the M_w: 100,000 PAA for the PP) was deposited as the last layer on the surface with similar procedure to provide shielding and attaching sites for possible further use.

Characterization

The core particle structure was determined at room temperature with the X-ray powder diffraction (XRD) using a Huber G670 image plate Guinier camera (Cu $K_{\alpha 1}$ radiation, 1.5406 Å) with a 2θ range of 4-100° (step 0.005°). Data collection time was 30 min and 10 data reading scans were collected from the image plate. From this data the crystallite size of the core material was calculated with the Scherrer formula[39] using reflections (002) and (200) for the thickness and width of the hexagonal faces, respectively.

The surface ions were probed with reflection spectra measured using Avantes Avaspec-2048×14 fiber spectrometer between 350 and 1000 nm. As a light source a 60 W incandescent light bulb was used and the measurements were done with integration time of 400 ms and 30 scans. The presence of the polyelectrolytes was studied with Fourier transformed infrared spectra (FT-IR) using Bruker Vertex 70 using MVP Star Diamond setup with 32 scans between 450 and 4500 cm^{-1}. The resolution was 4 cm^{-1}. The elemental composition of the products was studied with X-ray fluorescence spectroscopy (XRF) with PANanalytical Epsilon 1 apparatus using its internal Omnian calibration with four scans. The qualitative thermal behavior of the coated materials was

studied with a TA Instruments SDT Q600 TGA-DSC apparatus. The error for weight in this setup is ca. 1 %. The measurements were made between 35 and 600 °C with heating rate of 10 °C/min using flowing air sphere (100 ml/min). The zeta potential to evaluate surface coverage was measured with Malvern Zetasizer Nano-ZS equipment using three replicate measurements. The pH of the aqueous solutions was ca. 6 and the nanoparticle concentration 100 μg/ml. The images of the coated nanoparticles were obtained with JEM-1400 Plus transmission electron microscopy (TEM) using OSIS Quemesa 11 Mpix bottom mounted digital camera. The nanoparticles were suspended into ethanol and dried on lacey carbon grid and then imaged with acceleration of 60 kV. The upconversion luminescence spectra were measured at room temperature with an Avantes Avaspec HS-TEC spectrometer. A fiber-coupled continuous NIR laser diode IFC-975-008-F (Optical Fiber Systems) with excitation wavelength of 973 nm (10 270 cm^{-1}) was used as an excitation source with power density range of 3.2–11.1 Wcm^{-2}. Dry nanomaterials were held inside a rotating capillary tube. After the sample a short-pass filter with a cutoff of 750 nm (Newport) was used to exclude excitation radiation. The emission was collected at a 90° angle to the excitation and directed to the spectrometer with an optical fiber. The downshifted emission and excitation spectra were measured from a dry nanomaterial with a Varian Cary Eclipse spectrofluorometer. Phosphorescence mode with 0.1 ms delay and 0.5 ms gate time was used to record the spectra.

The time dependent upconversion luminescence decay measurements in aqueous media (particle concentration 5 μg/ml) were carried out using 980 nm excitation and a lifetime measurement mode with a modified Plate Chameleon fluorometer.[40] The luminescence decays were measured after incubating the nanoparticles for 0, 4 or 24 h in pure water or 5 mM phosphate buffer (pH 7.75) with or without 1 mM KF in slow shaking. The measurements were done in Greiner polypropylene microtiter plates. The samples were exposed repeatedly to 2 ms pulsed excitation and the emissions

were collected using 535/40 nm band-pass filter. Obtained data was analyzed using second-order exponential decay fitting of Origin 8 (OriginLab, Northampton, MA).

RESULTS AND DISCUSSION

Success of the coating process and coverage

The β-$NaYF_4$:Yb^{3+},Er^{3+} upconversion materials used for the layer-by-layer coating were prepared with the method described earlier[13] and were of hexagonal form with a size *ca*. 22*26 nm (Table S1). As the synthesis produces oleic acid capped nanoparticles, the oleic acid had to be removed before the coating. The removal was confirmed with the FT-IR spectra where it could be easily seen as a reduction of the asymmetric and symmetric vibrations of COO^- (Figure S1). After the oleic acid surface was removed the bare particles were used as a core for the coating process.

The FT-IR spectra showed that the desired polyelectrolytes were present in all of the coated materials (Figure S2). The strongest vibrations from PAA and PP could be distinguished at different sections in the recorded spectra, the main vibrations of PAA being around 1000–1750 cm^{-1} [1] and PP 900–1400 cm^{-1} [41]. No quantitative conclusions could be made from FT-IR spectra, but with the materials prepared with PAA M_w: 100,000 and both lengths of PP having three bilayers the polyelectrolyte related vibrations seemed to be the strongest (S2). This is a good indicator that there should be more polyelectrolyte present on the material. In addition, the reflectance spectroscopy revealed the presence of neodymium ions on the surface (Figure S3). The absorption of neodymium ions (575, 740, 795 and 870 nm) were easily distinguishable from the ones arising from the core lanthanide ions (490, 520, 540, 640 and 800 for Er^{3+} and 975 nm for Yb^{3+}) (Figure 1). The absorbance of neodymium ions was increased with the increasing number of bilayers and the increase of the PAA polyelectrolyte length, which implies successful layer formation. This was

expected as the longer PAA chain has more attaching sites to capture neodymium ions on to the structure.

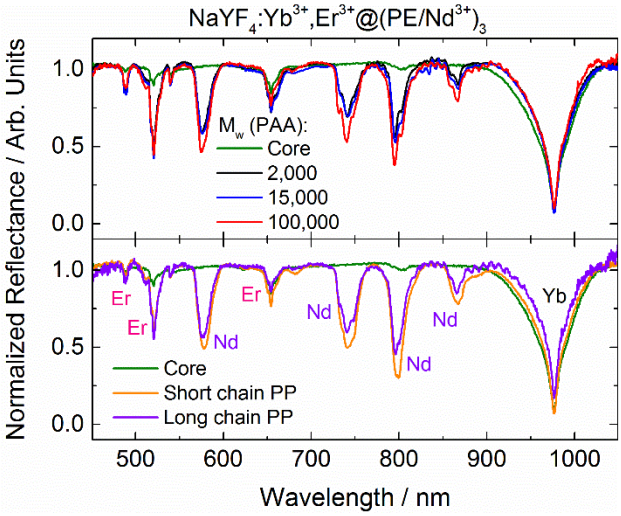

Figure 1. Reflectance spectra of the core and coated $NaYF_4:Yb^{3+},Er^{3++}@(PE/Nd^{3+})_3$ materials prepared with selected polyelectrolyte lengths PAA (M_w: 2,000; 15,000 and 100,000) and short and long chain PP.

The shorter chain PP seemed to be better in attaching the neodymium ions than the longer chain. The polymer chain is expected to be similarly open in all of the deposition solutions as the ionic concentration was unchanged.[42] In addition, the pH of the solutions was constant so the percentage of open attaching sites is expected to be similar in all polyelectrolytes.

The increase in the number of bilayers with PAA/Nd^{3+} should be seen as an increase in the weight loss during the thermal analysis (Figure S4). This was true with both M_w: 2,000 and 100,000 coated materials. In addition, the shape of the TGA curves of the second and third bilayer are different from that of the first bilayer suggesting that the bilayer formation is more defined due to increasing hydration layer (water) on the material surface. However, with the M_w: 15,000 the weight loss is

198 decreasing with increasing number of bilayers and the weight loss curve of the first bilayer behaves
199 differently from the others. It is possible that with this length of PAA the bilayer formation is not
200 sufficient at the first bilayers but only after further coating cycles. With short chain PP layers the
201 thermal analysis showed a decrease in the weight loss with increasing layers suggesting that more
202 polyphosphate is present in the materials as the polyphosphate should remain unaffected during
203 the heating (Figure 2, S4). The behavior in TGA curves with increasing number of bilayers is
204 similar to those obtained with fire-retardant ammonium polyphosphate[43] suggesting that the
205 bilayers shield the inner particle and possible remaining impurities in the structure making the
206 weight loss smaller. There is also possibility that the nearby neodymium ions interact with the
207 polyphosphate forming $Nd_3O_3PO_4$ that could contribute to the weight gain but its contribution is
208 expected to be minimal.

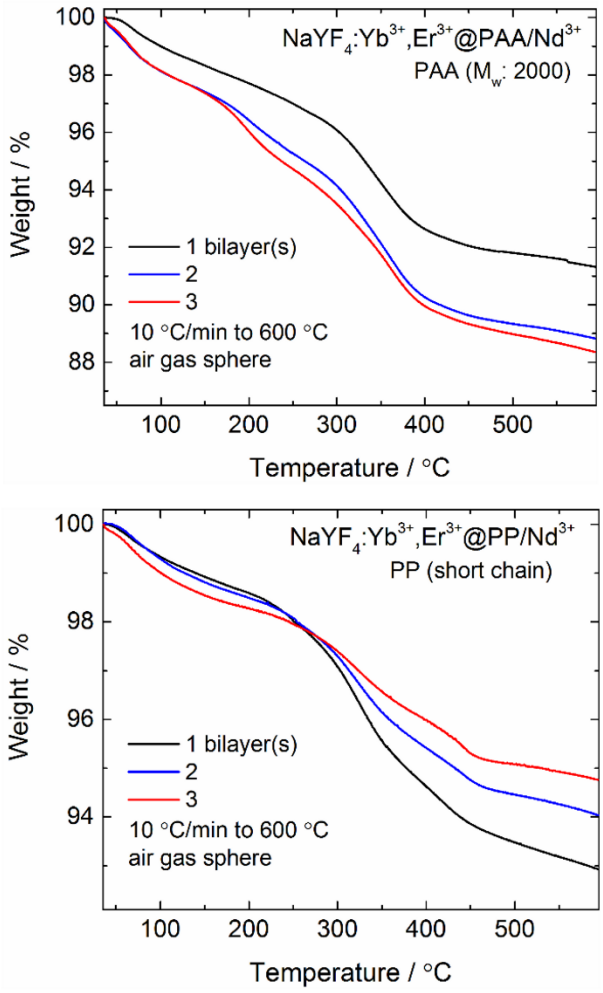

Figure 2. Thermal analysis of the $NaYF_4:Yb^{3+},Er^{3++}$@PAA/Nd^{3+} materials coated with M_w(PAA): 2,000 (top) and short chain polyphosphate (bottom) with deposition concentrations of 10 mM PP/PAA in 0.1 NaCl (aq) and 10 mM $NdCl_3$ (aq).

The increase of neodymium at the materials with the increase in the number of bilayers could be observed from the XRF measurements (Table S2, Figure S5). With varying PAA lengths the increase was linear but small. The only distinguishable difference observed was that, as with the reflectance spectroscopy, the longest polyelectrolyte was the most efficient in attaching the neodymium ions. With PP, the increase in neodymium amount was also linear. However, some

differences between the amounts of phosphorus were observed. With the short chain the increase was linear but with longer chain it could be debated that the increase after two bilayers indicates exponential growth in the amount of phosphorus. This could be attributed to the fact that longer polyphosphate chain could develop branched structures around the particle because the chain ends reaching out from particle surface are able to also host the next oppositely charged layer formation.

The zeta potential was used to observe differences in the surface charge with increasing number of bilayer formation. All of the core materials were observed to have similar zeta potential (*ca*. 20 mV) as reported previously from the bare upconversion nanoparticle core.[26] With all the materials the zeta potential decreased with increasing number of bilayers as expected. The positive charge arising from the Nd^{3+} ions is negligible in comparison to the negative charge of the polyelectrolytes. However, the zeta potential decrease between first and second bilayer was small, which suggests that even though the coating was observed it is possible that it might not occur linearly but with a step-like manner (Figure 3). With different lengths of PAA it was observed that the coating was most efficient during the first bilayer with the shortest polyelectrolyte (M_w (PAA): 2,000), as expected and the longer two (M_w (PAA): 15,000 and 100,000) behaved similarly during the first layer. When three bilayers were formed the smallest two seemed to form better coverage resulting in lower zeta potential (ca. -7 mV) than the longest PAA (*ca*. 3 mV). With polyphosphate used as a coating component the bilayer formation was also observed being similar to those with varying PAA lengths. The shorter polyphosphate seemed to cover more of the particle surface on the first bilayer but eventually both lengths of polyphosphate reached similar zeta potential of -5 mV at three bilayers (Figure S6). The zeta potential of all coated materials except the longest PAA reached between -5 and -10 mV at three bilayers suggesting that the coverage at that certain stage

could be similar regardless of the length of the polyelectrolyte or the pathway how each bilayer is formed.

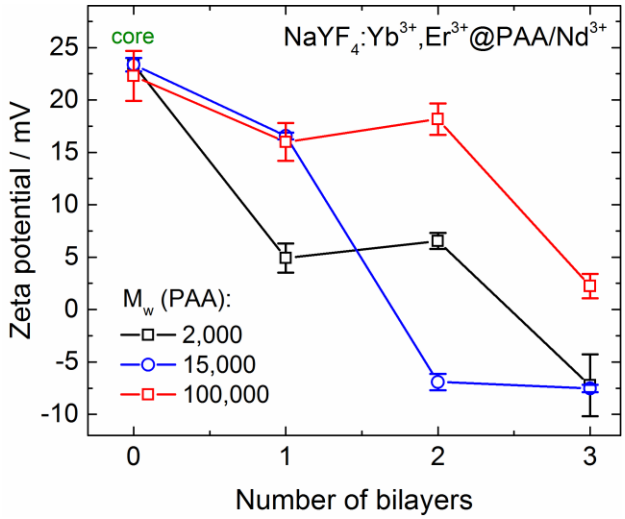

Figure 3. Zeta potential of the core and $NaYF_4:Yb^{3+},Er^{3+}$@PAA/Nd^{3+} materials coated with deposition concentrations of 10 mM PAA in 0.1 NaCl (aq) and 10 mM $NdCl_3$ (aq). The lines are only guide for the eye.

TEM imaging was used to probe if the bilayers were visible on the nanoparticle surface. To observe the delicate organic structure on the surface, the suspended materials were dried on the lacey carbon grid to minimize the background and imaged with low, 60 kV voltage. From the images some indication of the bilayers could be drawn as the surface of the materials is fuzzy and similar to those obtained previously (Figure 4).[35] The imaging grid and the used solvent can have an effect in aggregating the nanoparticles as they seem to attach to the carbon fiber edges. However, with this small number of bilayers it is unclear if the *ca*. 2 nm rings around the nanoparticles are actually the bilayers or combination of bilayers and solution boundaries.

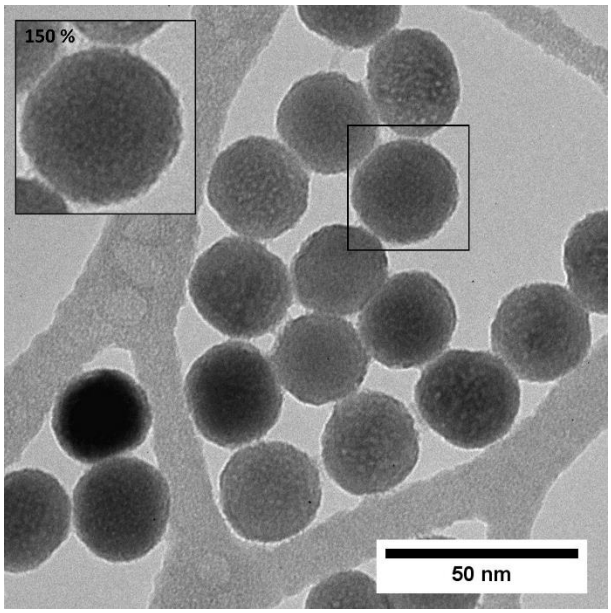

Figure 4. TEM image of the $NaYF_4:Yb^{3+},Er^{3+}@(PAA/Nd^{3+})_3$ materials coated with PAA M_w: 2,000. Scale bar is 50 nm, inset zoom is 150 %.

Luminescence properties

The upconversion luminescence of the coated nanoparticles was studied by 973 nm (10 280 cm^{-1}) excitation which is suitable for the well-known energy transfer upconversion from ytterbium ion to erbium.[44,45] The characteristic emission of Er^{3+} in green ($^2H_{11/2}$, $^4S_{3/2} \rightarrow {}^4I_{15/2}$) and red ($^4F_{9/2} \rightarrow {}^4I_{15/2}$) wavelength region was observed from all of the prepared materials.[45] With the materials coated with varying PAA lengths it was notable that with the shortest PAA (M_w: 2,000) the most intense upconversion luminescence was observed from the material with three bilayers (Figure S7). With others PAA lengths the first bilayer was found to be the most effective in shielding the luminescence. The strongest enhancement in comparison to the core material, *ca*. 2.5 times stronger, was observed with one bilayer of M_w: 15,000 PAA (Figure 5, top). With the varying lengths of PP similar enhancement was observed with lower bilayer amounts but the overall effect was weaker than with PAA.

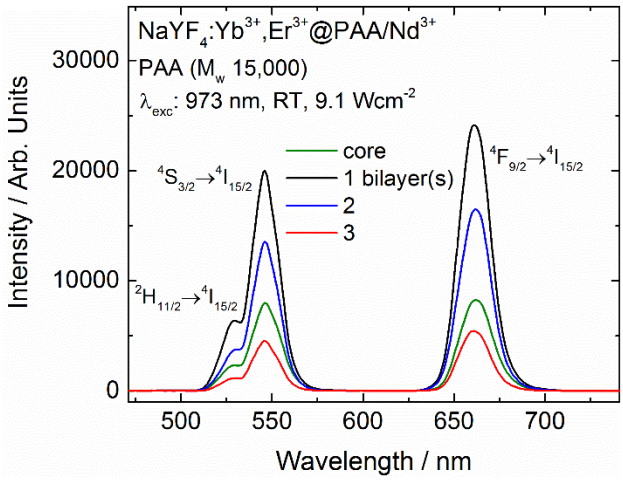

Figure 5. Upconversion luminescence spectra excited with 973 nm of the core and $NaYF_4:Yb^{3+},Er^{3+}$@PAA/Nd^{3+} materials coated with PAA M_w: 15,000.

When the intensity of emission from green and red energy levels is plotted against the excitation power density in a log-log plot its linearity gives information about the photons needed for the upconversion process. The obtained slopes for the green emission were *ca*. 2 indicating two-photon process as expected (Table S3). With the red emission the slopes were generally higher than previously achieved with oleic acid capped materials[13,46] and in some of the materials raised as high as *ca*. 2.5. With larger (*ca*. 90 nm) oleic acid capped particles this higher slope for red emission has been observed and is expected to be due to the back energy transfer process to the Yb^{3+} sensitizer.[44] In addition, the presence of H_2O molecules seems to increase the slope and lead to the population of the red emitting state via green emitting levels without the back transfer process.[45] To study this further, downshifted emission and excitation spectra were measured with varying excitation wavelengths to probe the possible pathway to the red upconversion luminescence (Figure S8). We observed that the red emission is obtained regardless of the excitation wavelength. With the spectra obtained from the materials prepared by Berry et al. and Hyppänen et al. both the excitation spectra of the materials dispersed in toluene and D_2O,

respectively, red emission lacked the component from the green emitting states of Er^{3+} ($^2H_{11/2}$, $^4S_{3/2}$).[44,45] However, with our dry materials these energy levels are clearly visible (Figure S9). In materials prepared with shorter PAA lengths (M_w: 2,000 and 15,000) the red emission has less input from the green emitting levels than from the bare core materials. In the case of longer PAA (M_w: 100,000) this difference is not so clear suggesting more involvement from H_2O molecules that are more easily interlocked into the longer polyelectrolyte structures. So we believe that in our materials the H_2O molecules play a significant role as the surface quencher[19] both in the oleic acid free core materials as well as in the coated materials because of the probability of interlocked H_2O molecules within the layer structure. This leads to the red emission using a combination of both two and three photon processes depending on the environment of the ytterbium and erbium ions confirming the obtained slope values for green and red emissions.

The time dependent behavior of the coated nanomaterials in water suspension was measured with a modified Plate Chameleon fluorometer using 980 nm excitation and detecting the green upconversion luminescence at 535 nm.[40] The emissions were collected directly after suspension to aqueous solution. After 2 ms wide pulsed excitation, the data was collected for 8 ms. The obtained data was fitted (after 50 μs to exclude the delayed energy transfer from Yb^{3+} to Er^{3+}) with second-order exponential decay function. It must be noted that the fitted decay times of the green emission arise from complex excitation and emission systems between the active ions as well as long-lived intermediate energy states and not only from the emitting energy levels of erbium.[47] When the lifetime components of the coated materials are compared with those of core materials it could be observed that there is a decrease especially in the first component with shorter polyelectrolyte chains. However, the changes in the second lifetime component for the PAA coated materials is reasonably small and for the longest PAA (M_w: 100,000) the decrease is negligible (Table 1, Table

S4, Figure S10). The difference between the lifetimes of the different core materials (and their coated products) is expected to arise from the size differences (*ca*. 20*25 and 23*29 nm) inducing differences in energy migration through ytterbium energy levels within the particles[47], as the larger particles' lifetimes are similar with those obtained previously.[20,45] It could be observed that the percentual share of the lifetime components shifts slightly to the second component after coating. This seems reasonable as the longer lifetime is thought to be connected to the inner Er^{3+} ions at the core that are more shielded from the environment.

Table 1. Upconversion luminescence lifetimes of the coated nanoparticles. The amplitude indicates the % effect in the total lifetime.

Sample	Polyelectrolyte	τ_1 / μs	A / %	τ_2 / μs	A / %
Core	-	71±1	94	668±21	6
1 bilayer	PAA M_w: 100 000	69±1	93	683±22	7
2 bilayers	"	69±1	92	636±21	8
3 bilayers	"	66±1	92	654±15	8

When the upconversion emission intensity during the time dependent measurements was studied in aqueous suspension with the shorter chains of PAA (M_w 2,000 and 15,000) the intensity did not change significantly when the core was coated. However, with the longest PAA (M_w 100,000) the upconversion luminescence intensity increased with the number of bilayers being strongest with two bilayers. With both lengths of polyphosphate, the emission intensity decreased after first bilayer suggesting that multiple bilayers did not help preserving the upconversion luminescence (Table S4, Figure S10).

Disintegration of the coated particles

The stability of the coating and possible disintegration of the coated particles was studied with upconversion luminescence decay measurements in three time points after suspension to liquid media. The disintegration of the nanoparticles can be observed through the changes in their emission both in intensity and in lifetime components already during the first hours after introducing them into aqueous buffers.[20,21] Adding 1 mM KF in aqueous suspension has been reported to hinder or even prevent the disintegration of the particles in most used buffers excluding the phosphate based buffers.[20] For this reason our measurements were conducted both in pure water and in phosphate buffer with or without the addition of 1 mM KF to observe differences in the behavior of the material's upconversion luminescence intensity and decay at time points 0, 4 and 24 h.

Without the addition of KF in pure water the detected emission at 535 nm decreased from 0 to 4 hours in all of the materials with PAA/Nd^{3+} bilayers but no significant decrease followed the remaining 24 hours. However, with the longest PAA (M_w: 100,000) coated with three bilayers of PAA/Nd^{3+} the overall emission decrease was smallest from the coated PAA materials during the measurement period (Figure 6, S11). This suggests that the bilayers shield the particle for the disintegration in water. Similar conclusion could be drawn when the lifetime components were considered (Figure S11, Table S5), the second lifetime decreased less from 4 to 24 hours than it does between 0 and 4 hours. Only with the longest PAA the second lifetime decreased less than 100 μs during the aging period confirming that the particle is shielded from the disintegration. As the second lifetime is thought to be connected to the inner core of the particles its significant decrease is considered as an indicator of disintregration.[20] With all of the materials coated with PAA/Nd^{3+} bilayers the addition of 1 mM KF in pure water prevented the emission decrease for 24 hours as expected. The small emission intensity increase especially in the core material

measurements is thought to arise from possible aggregation of the particles in the measurement well during the incubation periods.

Table 2. Upconversion luminescence lifetimes of the $(PAA/Nd^{3+})_3PAA$ -coated nanoparticles (M_w(PAA): 100,000) at 5 μg/ml measured at 0, 4 and 24 hours in water, water + 1 mM KF, phosphate buffer and phosphate buffer + 1 mM KF. The amplitude indicates the % effect in the total lifetime.

		H_2O	A / %	+ KF	A / %	Phosphate	A / %	+ KF	A / %
0 h	τ_1 / μs	66±1	92	67±1	92	67±1	92	68±1	92
	τ_2 / μs	654±11	8	657±14	8	655±14	8	664±15	8
4 h	τ_1 / μs	63±1	92	67±1	92	65±1	92	66±1	92
	τ_2 / μs	590±12	8	653±12	8	611±11	8	660±14	8
24 h	τ_1 / μs	62±1	92	65±1	92	91±1	92	67±1	92
	τ_2 / μs	578±13	8	638±12	8	[a]		620±12	8

[a] The phosphate buffer 24 h measurement could only be fitted reasonably with 1st order exponential decay.

When the PAA/Nd^{3+} coated nanomaterials were introduced into phosphate buffer their behavior changed from that when suspended pure water. In the phosphate buffer the signal remained similar until the 4 hour measurement and then decreased when 24 hours was achieved. The behavior of the second lifetime component is similar, suggesting that the phosphate cannot interfere with the particle structure within the time scale. In addition, when introduced in phosphate buffer with 1 mM KF the emission signal and the lifetime components could be maintained throughout the

whole 24 hour measurement window. This is an improvement to previous results where the various upconversion nanomaterials were seen to lose their luminescence intensity when introduced in phosphate buffer already in the first four hours of time course and this decrease happened even with the addition of KF in solution.[20,21]

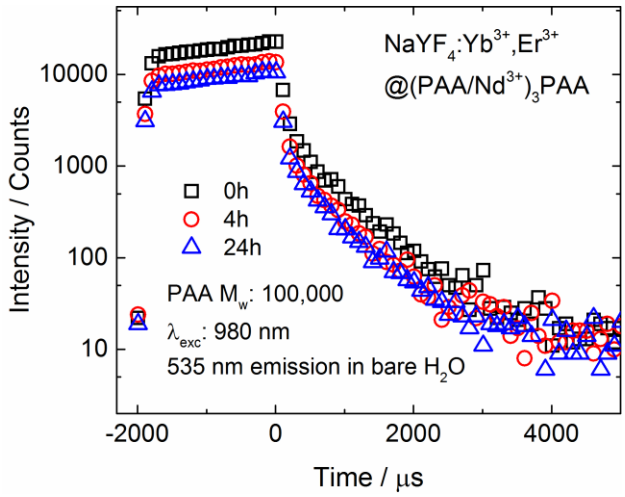

Figure 6. Upconversion luminescence decay spectra excited with 980 nm and detected at 535 nm at time steps 0, 4 and 24 h for $NaYF_4:Yb^{3+},Er^{3+}$@$(PAA/Nd^{3+})_3$PAA material (M_w: 100,000) measured in pure water.

With both lengths of polyphosphate similar behavior to those with PAA/Nd^{3+} bilayers was observed with and without the 1 mM KF addition into solution (Figure S11, Table S5). Only the first bilayer of PP/Nd^{3+} with short PP was able to shield the emission and disintegration for the first 4 hours of measurement in pure water. In all other cases, the emission decreased significantly already during that time period. The addition of 1 mM KF into the measurement solutions was able to prevent the emission decrease in the pure water-based measurements except with the additional number of bilayers of short polyphosphate. With measurements in phosphate buffer the bilayers prepared with longer polyphosphate were able to shield the emission intensity for the first

4 hours as with the PAA/Nd^{3+} bilayers. Only the first bilayer of PP/Nd^{3+} with short polyphosphate was similar to that of long polyphosphate, with increasing number of bilayers of the short polyphosphate the emission decreased significantly. In the phosphate buffer based measurements the 1 mM KF addition was effective only with the materials coated with longer polyphosphate, suggesting that the short polyphosphate in the bilayers interacts and detaches faster when in contact with the buffer solution.

CONCLUSIONS

We have demonstrated that using various lengths of polyelectrolytes the layer-by-layer method can be utilized for surface passivation and can offer further functionalization of upconverting nanoparticles. In addition, we observed that selected bilayer formations were able to shield the upconversion luminescence and thus prevent the disintegration of the nanoparticles even in the phosphate buffer that has been proven to enhance the disintegration.[20,21,48]

Overall, the modifications made with poly(acrylic acid) showed better bilayer formation than those made with polyphosphate. The length of the used polyelectrolytes had most influence on the first formed bilayer but with increasing number of bilayers the effects leveled. The most efficient enhancement to overall upconversion luminescence intensity was obtained with the first bilayer of PAA/Nd^{3+} prepared with PAA M_w: 15,000. The coating with short PP had a negative effect on the upconversion luminescence lifetimes while others showed no significant decrease in the lifetime components.

The disintegration of the nanoparticles was investigated with both pure water and the phosphate buffer for 24 hours. It was observed that with selected number of bilayers of PAA/Nd^{3+} the disintegration in pure water could be prevented without additional fluoride during the whole 24

hour investigation. Also, all of the materials excluding short polyphosphate showed resistance to disintegration for the first four hours when introduced in the phosphate buffer. Addition of 1 mM KF into the phosphate buffer solution was also able to prevent the disintegration and emission intensity loss during the measurement window.

The results presented in this study provide new pathways for the design of upconverting nanoparticles and their surface modifications. While we acknowledge that more studies are needed in both the layer-by-layer process and the layer stability in these kind of hybrid materials in the future, we also believe that this research brings additional possibilities to find a solution to hinder and prevent the disintegration of these delicate nanoparticles especially in the phosphate buffer based aqueous environments.

SUPPORTING INFORMATION

Additional characterization data for materials (FT-IR spectra, reflection spectra, XRF analysis, thermal analysis, upconversion luminescence spectra and decay studies) are available in the supporting information.

ACKNOWLEDGEMENT

Financial support to EP from the Vilho, Yrjö and Kalle Väisälä Foundation and Turku University foundation is gratefully acknowledged. Ermei Mäkilä is thanked for the help during the zeta potential measurements and Markus Peurla for the TEM images. This work made use of the Laboratory of Electron Microscopy premises at University of Turku.

REFERENCES

(1) Auzel, F. Upconversion and Anti-Stokes Processes with f and d Ions in Solids. *Chem. Rev.* **2004**, *104*, 139–173.

(2) Shan, G. Bin; Assaaoudi, H.; Demopoulos, G. P. Enhanced Performance of Dye-Sensitized Solar Cells by Utilization of an External, Bifunctional Layer Consisting of Uniform β-$NaYF_4$:$Er^{3+}Yb^{3+}$ Nanoplatelets. *ACS Appl. Mater. Interfaces* **2011**, *3*, 3239–3243.

(3) Shang, Y.; Hao, S.; Yang, C.; Chen, G. Enhancing Solar Cell Efficiency Using Photon Upconversion Materials. *Nanomaterials* **2015**, *5*, 1782–1809.

(4) Zhou, J.; Liu, Q.; Feng, W.; Sun, Y.; Li, F. Upconversion Luminescent Materials : Advances and Applications. *Chem. Rev.* **2015**, *115*, 395–465.

(5) Arppe, R.; Näreoja, T.; Sami, N.; Mattson, L.; Koho, S.; Rosenholm, J. M.; Soukka, T.; Schäferling, M. Photon Upconversion Sensitized Nanoprobes for Sensing and Imaging of pH Sensing and Imaging of pH. *Nanoscale* **2014**, *6*, 6837–6843.

(6) Chen, G.; Qiu, H.; Prasad, P. N.; Chen, X. Upconversion Nanoparticles: Design, Nanochemistry, and Applications in Theranostics. *Chem. Rev.* **2014**, *114*, 5161–5214.

(7) Guo, H.; Sun, S. Lanthanide-Dopd Upconverting Phosphors for Bioassay and Therapy. *Nanoscale* **2012**, *4*, 6692–6706.

(8) Ylihärsilä, M.; Valta, T.; Karp, M.; Hattara, L.; Harju, E.; Hölsä, J.; Saviranta, P.; Waris, M.; Soukka, T. Oligonucleotide Array-in-Well Platform for Detection and Genotyping Human Adenoviruses by Utilizing Upconverting Phosphor Label Technology. *Anal. Chem.* **2011**, *83*, 1456–1461.

(9) Arppe, R.; Mattsson, L.; Korpi, K.; Blom, S.; Wang, Q.; Riuttamäki, T.; Soukka, T. Homogeneous Assay for Whole Blood Folate Using Photon Upconversion. *Anal. Chem.*

2015, *87*, 1782–1788.

(10) Haase, M.; Schäfer, H. Upconverting Nanoparticles. *Angew. Chemie - Int. Ed.* **2011**, *50*, 5808–5829.

(11) Wilhelm, S.; Kaiser, M.; Würth, C.; Heiland, J.; Carrillo-Carrion, C.; Muhr, V.; Wolfbeis, O. S.; Parak, W. J.; Resch-Genger, U.; Hirsch, T. Water Dispersible Upconverting Nanoparticles: Effects of Surface Modification on Their Luminescence and Colloidal Stability. *Nanoscale* **2015**, *7*, 1403–1410.

(12) Rinkel, T.; Raj, A. N.; Dühnen, S.; Haase, M. Synthesis of 10 nm β-$NaYF_4$:Yb,Er/$NaYF_4$ Core / Shell Upconversion Nanocrystals with 5 nm Particle Cores. *Angew. Chemie - Int. Ed.* **2016**, *55*, 1164–1167.

(13) Palo, E.; Tuomisto, M.; Hyppänen, I.; Swart, H. C.; Hölsä, J.; Soukka, T.; Lastusaari, M. Highly Uniform Up-Converting Nanoparticles: Why You Should Control Your Synthesis Even More. *J. Lumin.* **2017**, *185*, 125–131.

(14) Krämer, K. W.; Biner, D.; Frei, G.; Güdel, H. U.; Hehlen, M. P.; Lü; Thi, S. R. Hexagonal Sodium Yttrium Fluoride Based Green and Blue Emitting Upconversion Phosphors. *Chem. Mater.* **2004**, *16* (7), 1244–1251.

(15) Sommerdjik, J. L. On the Excitation Mechanisms of the Infrared-Exited Visible Luminescence in Yb^{3+}, Er^{3+}-Doped Fluorides. *J. Lumin.* **1971**, *4*, 441–449.

(16) Suyver, J. F.; Grimm, J.; Veen, M. K. Van; Biner, D.; Krämer, K. W.; Güdel, H. U. Upconversion Spectroscopy and Properties of $NaYF_4$ Doped with Er^{3+}, Tm^{3+} and/or Yb^{3+}. *J. Lumin.* **2006**, *117*, 1–12.

(17) Harju, E.; Hyppänen, I.; Hölsä, J.; Kankare, J.; Lahtinen, M.; Lastusaari, M.; Pihlgren, L.; Soukka, T. Polymorphism of $NaYF_4$:Yb^{3+},Er^{3+} Up-Conversion Luminescence Materials.

Z. Krist. Proc. **2011**, *1*, 381–387.

(18) Gorris, H. H.; Resch-Genger, U. Perspectives and Challenges of Photon-Upconversion Nanoparticles - Part II Bioanalytical Applications. *Anal. Bioanal. Chem.* **2017**, *409*, 5875–5890.

(19) Arppe, R.; Hyppanen, I.; Perälä, N.; Peltomaa, R.; Kaiser, M.; Würth, C.; Christ, S.; Resch-Genger, U.; Schäferling, M.; Soukka, T. Quenching of the Upconversion Luminescence of $NaYF_4:Yb^{3+},Er^{3+}$ and $NaYF_4:Yb^{3+},Tm^{3+}$ Nanophosphors by Water: The Role of the Sensitizer Yb^{3+} in Non-Radiative Relaxation. *Nanoscale* **2015**, *7*, 11746–11757.

(20) Lahtinen, S.; Lyytikäinen, A.; Päkkilä, H.; Hömppi, E.; Perälä, N.; Lastusaari, M.; Soukka, T. Disintegration of Hexagonal $NaYF_4:Yb^{3+}$,Er^{3+} Upconverting Nanoparticles in Aqueous Media: The Role of Fluoride in Solubility Equilibrium. *J. Phys. Chem. C* **2017**, *121*, 656–665.

(21) Plohl, O.; Kraft, M.; Kovac, J.; Belec, B.; Ponikvar-Svet, M.; Würth, C.; Lisjak, D.; Resch-Genger, U. Optically Detected Degradation of $NaYF_4$:Yb,Tm-Based Upconversion Nanoparticles in Phosphate Buffered Saline Solution. *Langmuir* **2017**, *33*, 553–560.

(22) Johnson, N. J. J.; Korinek, A.; Dong, C.; Veggel, F. C. J. M. Van. Self-Focusing by Ostwald Ripening : A Strategy for Layer-by- Layer Epitaxial Growth on Upconverting Nanocrystals. *J. Am. Chem. Soc.* **2012**, *134*, 11068–11071.

(23) Zhong, Y.; Tian, G.; Gu, Z.; Yang, Y.; Gu, L.; Zhao, Y.; Ma, Y. Elimination of Photon Quenching by a Transition Layer to Fabricate a Quenching-Shield Sandwich Structure for 800 Nm Excited Upconversion Luminescence of Nd^{3+} - Sensitized Nanoparticles. *Adv. Mater.* **2014**, *26*, 2831–2837.

(24) Li, Z.; Wang, L.; Wang, Z.; Liu, X.; Xiong, Y. Modification of $NaYF_4$:Yb,Er@SiO_2 Nanoparticles with Gold Nanocrystals for Tunable Green-to-Red Upconversion Emissions. *J. Phys. Chem. C* **2011**, *115*, 3291–3296.

(25) Chen, X.; Zhou, D.; Xu, W.; Zhu, J.; Pan, G.; Yin, Z.; Wang, H.; Zhu, Y.; Shaobo, C.; Song, H. Fabrication of Au-Ag nanocage@$NaYF_4$@$NaYF_4$:Yb,Er Core- Shell Hybrid and Its Tunable Upconversion Enhancement. *Sci. Rep.* **2017**, *7*, 41079.

(26) Plohl, O.; Kralj, S.; Majaron, B.; Fröhlich, E.; Ponikvar-svet, M.; Makovec, D.; Lisjak, D. Amphiphilic Coatings for the Protection of Upconverting Nanoparticles against Dissolution in Aqueous Media. *Dalt. Trans.* **2017**, *46*, 6975–6984.

(27) Xiao, H.; Li, F.; Zhang, Z.; Feng, L.; Li, Z.; Yang, J.; Chai, Z. Distribution of Ytterbium-169 in Rat Brain after Intravenous Injection. *Toxicol. Lett.* **2005**, *155*, 247–252.

(28) Agalakova, N. I.; Gusev, G. P. Molecular Mechanisms of Cytotoxicity and Apoptosis Induced by Inorganic Fluoride. *ISRN Cell Biol.* **2012**, 403835.

(29) Decher, G. Fuzzy Nanoassemblies: Toward Layered Polymeric Multicomposites. *Science* **1997**, *277* (5330), 1232–1237.

(30) Borges, J.; Mano, J. F. Molecular Interactions Driving the Layer-by-Layer Assembly of Multilayers. *Chem. Rev.* **2014**, *114*, 8883–8942.

(31) Schneider, G.; Decher, G. Functional Core/shell Nanoparticles via Layer-by-Layer Assembly. Investigation of the Experimental Parameters for Controlling Particle Aggregation and for Enhancing Dispersion Stability. *Langmuir* **2008**, *24*, 1778–1789.

(32) Hong, X.; Li, J.; Wang, M.; Xu, J.; Guo, W.; Li, J.; Bai, Y.; Li, T. Fabrication of Magnetic Luminescent Nanocomposites by a Layer-by-Layer Self-Assembly Approach. *Chem. Mater.* **2004**, *16*, 4022–4027.

(33) Salomäki, M.; Räsänen, M.; Leiro, J.; Huti, T.; Tenho, M.; Lukkari, J.; Kankare, J. Oxidative Inorganic Multilayers for Polypyrrole Film Generation. *Adv. Funct. Mater.* **2010**, *20*, 2140–2147.

(34) Salomäki, M.; Myllymäki, O.; Hätönen, M.; Savolainen, J.; Lukkari, J. Layer-by-Layer Assembled Oxidative Films as General Platform for Electrodeless Formation of Conducting Polymers. *ACS Appl. Mater. Interfaces* **2014**, *6*, 2325–2334.

(35) Palo, E.; Salomäki, M.; Lastusaari, M. Surface Modification of Upconverting Nanoparticles by Layer-by-Layer Assembled Polyelectrolytes and Metal Ions. *J. Colloid Interface Sci.* **2017**, *508*, 137–144.

(36) Prorok, K.; Bednarkiewicz, A. Energy Migration Up-Conversion of Tb^{3+} in Yb^{3+} and Nd^{3+} Codoped Active-Core/Active-Shell Colloidal Nanoparticles. *Chem. Mater.* **2016**, *28*, 2295–2300.

(37) Xie, X.; Gao, N.; Deng, R.; Sun, Q.; Xu, Q.; Liu, X. Mechanistic Investigation of Photon Upconversion in Nd^{3+}-Sensitized Core-Shell Nanoparticles. *J. Am. Chem. Soc.* **2013**, *135*, 12608–12611.

(38) Bogdan, N.; Vetrone, F.; Ozin, G. A.; Capobianco, J. A. Synthesis of Ligand-Free Colloidally Stable Water Dispersible Brightly Luminescent Lanthanide-Doped Upconverting Nanoparticles. *Nano Lett.* **2011**, *11*, 835–840.

(39) Klug, H. P.; Alexander, L. E. *X-Ray Powder Diffraction Procedures*; Wiley: New York, 1959.

(40) Soukka, T.; Kuningas, K.; Rantanen, T.; Haaslahti, V.; Lövgren, T. Photochemical Characterization of up-Converting Inorganic Lanthanide Phosphors as Potential Labels. *J. Fluoresc.* **2005**, *15*, 513–528.

(41) Workman, Jerry, J. *The Handbook of Organic Compounds: NIR, IR, Raman and UV-VIS Spectra Featuring Polymers and Surfactants*; Academic Press, 2001.

(42) Chodanowski, P.; Stoll, S. Polyelectrolyte Adsorption on Charged Particles in the Debye-Hueckel Approximation. A Monte Carlo Approach. *Macromolecules* **2001**, *34*, 2320–2328.

(43) Levchik, S. V.; Costa, L.; Camino, G. Effect of the Fire-Retardant Ammonium Polyphosphate on the Thermal Decomposition of Aliphatic Polyamides. Part III - Polyamides 6.6. and 6.10. *Polym. Degrad. Stab.* **1994**, *43*, 43–54.

(44) Berry, M. T.; May, P. S. Disputed Mechanism for NIR-to-Red Upconversion Luminescence in $NaYF_4:Yb^{3+}$,Er^{3+}. *J. Phys. Chem. A* **2015**, *119*, 9805–9811.

(45) Hyppänen, I.; Höysniemi, N.; Arppe, R.; Schäferling, M.; Soukka, T. Environmental Impact on the Excitation Path of the Red Upconversion Emission of Nanocrystalline $NaYF_4:Yb^{3+},Er^{3+}$. *J. Phys. Chem. C* **2017**, *121*, 6924–6929.

(46) Kaiser, M.; Würth, C.; Kraft, M.; Hyppänen, I.; Soukka, T.; Resch-Genger, U. Power-Dependent Upconversion Quantum Yield of $NaYF_4:Yb^{3+},Er^{3+}$ Nano- and Micrometer-Sized Particles - Measurements and Simulations. *Nanoscale* **2017**, *9*, 10051–10058.

(47) Hossan, Y.; Hor, A.; Luu, Q.; Smith, S. J.; May, P. S.; Berry, M. T. Explaining the Nanoscale Effect in the Upconversion Dynamics of β‑$NaYF_4:Yb^{3+}$, Er^{3+} Core and Core−Shell Nanocrystals. *J. Phys. Chem. C* **2017**, *121*, 16592–16606.

(48) Lisjak, D.; Plohl, O.; Vidmar, J.; Majaron, B.; Ponikvar-svet, M. Dissolution Mechanism of Upconverting AYF_4:Yb,Tm (A = Na or K) Nanoparticles in Aqueous Media. *Langmuir* **2016**, *32*, 8222–8229.

574 **TABLE OF CONTENTS:**

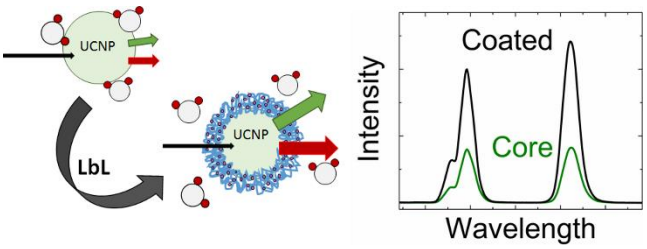

575